Photoreceptor Structure and Function in Patients with Congenital Achromatopsia

Mohamed A. Genead,[1,2] Gerald A. Fishman,[1,2] Jungtae Rha,[3] Adam M. Dubis,[4] Daniela Maria O. Bonci,[4,5] Alfredo Dubra,[6] Edwin M. Stone,[7] Maureen Neitz,[8] and Joseph Carroll[3,4]

PURPOSE. To assess photoreceptor structure and function in patients with congenital achromatopsia.

METHODS. Twelve patients were enrolled. All patients underwent a complete ocular examination, spectral-domain optical coherence tomography (SD-OCT), full-field electroretinographic (ERG), and color vision testing. Macular microperimetry (MP; in four patients) and adaptive optics (AO) imaging (in nine patients) were also performed. Blood was drawn for screening of disease-causing genetic mutations.

RESULTS. Mean ($\pm$SD) age was 30.8 ($\pm$16.6) years. Mean best-corrected visual acuity was 0.85 ($\pm$0.14) logarithm of the minimal angle of resolution (logMAR) units. Seven patients (58.3%) showed either an absent foveal reflex or nonspecific retinal pigment epithelium mottling to mild hypopigmentary changes on fundus examination. Two patients showed an atrophic-appearing macular lesion. On anomaloscopy, only 5 patients matched over the entire range from 0 to 73. SD-OCT examination showed a disruption or loss of the macular inner/outer segments (IS/OS) junction of the photoreceptors in 10 patients (83.3%). Seven of these patients showed an optically empty space at the level of the photoreceptors in the fovea. AO images of the photoreceptor mosaic were highly variable but significantly disrupted from normal. On ERG testing, 10 patients (83.3%) showed evidence of residual cone responses to a single-flash stimulus response. The macular MP testing showed that the overall mean retinal sensitivity was significantly lower than normal (12.0 vs. 16.9 dB, $P < 0.0001$).

CONCLUSIONS. The current approach of using high-resolution techniques to assess photoreceptor structure and function in patients with achromatopsia should be useful in guiding selection of patients for future therapeutic trials as well as monitoring therapeutic response in these trials. (*Invest Ophthalmol Vis Sci.* 2011;52:7298–7308) DOI:10.1167/iovs.11-7762

Congenital achromatopsia is a genetically heterogeneous, predominantly autosomal recessive, retinal disorder with a prevalence of approximately 1 in 30,000 in the general population.[1] It is characterized by a lack of color discrimination, poor visual acuity, photophobia, pendular nystagmus, and abnormal photopic electroretinographic (ERG) recordings with preservation of the rod-mediated ERG. A prior report by Khan and colleagues[2] showed that the rod ERG function can be modestly subnormal. The disease has been categorized into complete and incomplete achromatopsia subtypes. The incomplete (atypical) form is defined as dyschromatopsia, in which the symptoms are similar to those of the complete achromatopsia (typical) form but with less visual dysfunction.[3] Patients with the complete form have nondetectable cone function on ERG testing, whereas those with the incomplete form retain some residual cone function on ERG, and often more preserved color vision and a higher level of visual acuity (up to 0.20).[3–5] Funduscopy is usually normal in both forms, although not infrequently macular pigmentary mottling and even occasionally atrophic changes have been described.[6]

The known causes of congenital achromatopsia are all due to malfunction of the retinal phototransduction pathway. Specifically, recessive forms of achromatopsia result from the inability of cone photoreceptors to properly respond to a light stimulus by hyperpolarizing. To date, mutations in four genes have been identified to cause achromatopsia in human patients, including the α- and β-subunits of the cone cyclic nucleotide-gated ion channels, *CNGA3* (ACHM2, OMIM600053) and *CNGB3* (ACHM3, OMIM605080), which are located in the plasma membrane of the cone outer segments, the α-subunit of the cone photoreceptor transducin, *GNAT2* (ACHM4, OMIM139340), and the catalytic α-subunit of the cone cyclic nucleotide phosphodiesterase, *PDE6C* (OMIM600827). The vast majority of human cases of achromatopsia are caused by mutations in either *CNGA3* or *CNGB3*.[7–11] Prior recent reports of animal studies showed that *CNGB3*, *CNGA3*, or *GNAT2* knockout mice and naturally occurring dog models of achromatopsia responded well to adenoassociated

virus (AAV) gene therapy. In animal models of human achromatopsia, cone ERG amplitudes recovered to nearly normal levels.[12–14] These results from proof-of-principle experiments in animals with cone-directed gene therapy offer promise for eventual translation to human patients. Identifying and then targeting retinal locations with retained photoreceptors will be a prerequisite for successful gene therapy in achromatopsia patients.

Previous observations regarding photoreceptor structure in achromatopsia have been limited primarily to histologic reports. In a previous report by Galezowski,[15] the retinal cones were described as entirely absent. Larsen[16] reported malformed foveal cones with normal cones in the peripheral retina, whereas Harrison et al.[17] found misshaped and reduced numbers of retinal cones. In another report by Falls et al.,[18] normal numbers of odd-shaped foveal cones and isolated numbers of cones in the peripheral retina were described. Glickstein and Heath[19] found no evidence of foveal cones and reduced numbers of peripheral cones. Although genetic testing was not available at the time of these studies, they nevertheless highlight the fact that the picture of photoreceptor structure in achromatopsia is likely to be complex. Some clarity on this issue has begun to come from the use of noninvasive imaging techniques to assess photoreceptor structure in patients with achromatopsia. Optical coherence tomography (OCT), which provides excellent axial resolution, has been used to show a highly variable phenotype at the level of the photoreceptor inner segment (IS) and outer segment (OS),[4,6,20,21] although the general interpretation has been that there is an absence or reduction of healthy cone structure. Adaptive optics (AO) provides high lateral resolution,[22–24] and was used in a single case to examine photoreceptor structure on the single-cell level.[25] The authors visualized a normal rod photoreceptor mosaic, but did not report any evidence of cone structure. These findings only confirm the complexity of the photoreceptor phenotype in achromatopsia, thus warranting further investigation.

Here we used noninvasive high-resolution imaging tools (spectral domain [SD]-OCT and AO scanning laser ophthalmoscopy [SLO]) together with functional measures of vision (ERG, microperimetry [MP], and color vision) to assess photoreceptor structure and function in patients with congenital achromatopsia. We sought to correlate these findings with genetic information from the same subjects. Not only is this approach expected to provide a better understanding of the disease, but also should prove useful in identifying which patients may be most likely to benefit from participating in future gene-targeted treatment trials to rescue or restore cone photoreceptors in this group of patients. Moreover, the structural and functional assays used here would be useful for evaluating the therapeutic efficacy in patients who in fact go on to receive intervention.

METHODS AND MATERIALS

Participants

Twelve patients (24 eyes) with congenital achromatopsia were included in the study: 7 males (58.3%) and 5 females (41.7%). The mean ($\pm$SD) age of the patients was 30.8 ($\pm$16.6) years, with a range from 13 to 55 years. There were 6 Caucasian (50.0%), 2 Hispanic (16.7%), 3 of Middle Eastern ancestry (25.0%) (2 Jordanian, 1 Lebanese), and 1 African American (8.3%) enrolled in the study. Informed consent was obtained from all participants. All study patients underwent a complete ocular examination, SD-OCT, full-field ERG, color vision testing, macular MP (in 4 patients), and AO imaging (in 9 patients). Blood was drawn for screening of disease-causing genetic mutations.

The clinical testing portion of the study was conducted in the Department of Ophthalmology at the University of Illinois at Chicago and the Chicago Lighthouse for People Who Are Blind or Visually Impaired, whereas the AO imaging and additional OCT measurements were performed in the Department of Ophthalmology at the Medical College of Wisconsin. The screening for genetic mutations was performed by the Carver Nonprofit Genetic Testing Laboratory at the University of Iowa and additionally at both the Medical College of Wisconsin and the University of Washington. The present study followed the tenets of the Declaration of Helsinki and it was approved by institutional review boards at the University of Illinois, the Medical College of Wisconsin, and the University of Washington.

The diagnosis of achromatopsia was based on the history of a decrease in central vision, photophobia, markedly impaired color vision, nystagmus within the first decade of life, and abnormal cone responses on ERG recordings with most often normal, but occasionally subnormal, rod responses. Patients with a diagnosis of achromatopsia who were seen from August 2008 through February 2011 by two of the authors (MAG and GAF) during their routine clinical follow-up examinations were included in the current prospective study if they were willing to undergo the study protocol testing. Additional patients previously seen by one of the authors (GAF) were contacted by telephone and asked to participate in the study based on their prior diagnosis of achromatopsia.

Exclusion criteria included an inability to maintain moderately steady fixation, posterior uveitis, diabetic retinopathy, optic neuropathies, spherical refraction of more than ±6 diopters (D) or cylinder refraction of ±2D, or any central media opacity sufficient to hinder OCT and/or AO examinations. No patients with a history of any systemic diseases such as hypertension or diabetes mellitus were included. A summary of tests performed on each subject is given in Table 1.

Ocular Examination

Complete eye examination included best-corrected visual acuity (BCVA) using an Early Treatment Diabetic Retinopathy Study (ETDRS) chart (The Lighthouse, Long Island City, NY), slit-lamp biomicroscopic examination of the anterior segment, and intraocular pressure measurement with applanation tonometry (Goldmann; Haag-Streit USA, Mason, OH). Both eyes were dilated with 2.5% phenylephrine and 1% tropicamide. Fundus examination was performed using both direct and indirect ophthalmoscopy as well as biomicroscopy with a noncontact 78D lens.

ERG Examination

A full-field ERG was obtained monocularly with the use of a unipolar contact lens electrode (Burian Allen ERG Electrode; Hansen Ophthalmic Development Lab, Coralville, IA). One eye was tested after pupil dilation. The ERG responses were obtained according to the International Society for Clinical Electrophysiology of Vision guidelines[26] that included a dark-adapted rod-isolated response, a dark-adapted rod-dominant response, 32-Hz flicker response, and a light-adapted single-flash response. Parameters included amplitudes and implicit times for each of the major waveform components. All results were compared with 90% tolerance limits or an appropriate range for a visually normal population.

Color Vision Testing

All study patients underwent testing by using pseudoisochromatic plates (PseudoIsochromatic Plate Ishihara Compatible; T. Waggoner Inc., Gulf Breeze, FL) and Rayleigh match (Oculus Heidelberg Multi-Color Anomaloscope; Oculus Optikgeräte GmbH, Wetzlar, Germany), in which patients were asked to match a yellow monochromatic light in one test field of a bipartite stimulus with a mixture of various proportions of green and red lights in another portion of the bipartite field, by varying the proportion in the color mix. The average normal width of the Rayleigh match was about 2 units with a range of 5 units;

TABLE 1. Summary of Structural and Functional Findings in the Study Cohort

Patient Number	Visual Acuity (log MAR) OD	OS	Fundus Macular Appearance	Color Vision (Anomaloscope)	Full-field ERG Scotopic	Photopic Single-flash b-wave Amplitude	32-Hz Flicker	SD-OCT	AO Cone Structure	MP (dB)
1	0.92	0.90	wnl (OU)	Matched (0–73)	Normal	ND	ND	Normal IS/OS in the fovea	N/A	N/A
2	0.94	0.92	blunted FR (OU)	Matched (47–73)	Normal	Severely reduced	ND	Focal IS/OS disruption (small bubble) in the fovea	Minimal cone IS structure, no visible OS reflection	OD = 10.0 OS = 11.3
3	0.46	0.44	blunted FR (OU)	Matched (0–73)	Normal	Severely reduced	ND	Focal IS/OS disruption in the fovea + foveal hypoplasia	Moderate cone IS structure, no visible OS reflection	OD = 11.4 OS = 12.2
4	0.78	0.80	blunted FR (OU)	Matched (48–73)	Mildly reduced amplitude	Severely reduced	ND	IS/OS loss and disruption (large bubble) in the fovea	Minimal cone IS structure, no visible OS reflection	N/A
5	0.94	0.90	blunted FR (OU)	Matched (0–73)	Normal	ND	ND	Focal IS/OS disruption in the fovea (small bubble) + foveal hypoplasia	Substantial cone IS structure, frequent dim OS reflection	N/A
6	0.92	0.90	wnl (OU)	Matched (35–73)	Normal	Severely reduced	ND	Normal IS/OS in the fovea	Moderate cone IS structure, no visible OS reflection	OD = 11.6 OS = 12.5
7	0.92	0.96	Central foveal hypopigmentation with mild RPE mottling (OU)	Matched (0–73)	Normal	Severely reduced	ND	IS/OS loss (large bubble) in the fovea	No visible cone IS structure	N/A
8	0.80	0.72	Atrophic macular lesion (OU)	Matched (46–73)	Normal	Severely reduced	ND	Loss and disruption of IS/OS and RPE loss and thinning in the fovea + foveal hypoplasia	Minimal cone IS structure, no visible OS reflection	N/A
9	0.86	0.88	blunted FR (OU)	Matched (0–73)	Normal	Moderately reduced	ND	Loss and disruption of IS/OS (large bubble) in the fovea	N/A	N/A
10	0.94	0.82	Hypopigmented lesions with mild RPE mottling, punctuate drusen (OU)	Matched (49–73)	Moderately reduced amplitude	Severely reduced	ND	Focal loss and disruption of IS/OS and mild RPE thinning in the fovea + foveal hypoplasia	Minimal cone IS structure, occasional dim OS reflection	N/A
11	0.92	0.94	Atrophic macular lesion (OU)	Matched (10–73)	Moderately reduced amplitude	Severely reduced	ND	Loss of IS/OS and RPE loss and thinning in the fovea + foveal hypoplasia	N/A	N/A
12	0.92	0.90	wnl (OU)	Matched (41–73)	Normal	Severely reduced	ND	Focal loss of IS/OS + foveal hypoplasia	Substantial cone IS structure, occasional dim OS reflection	OD = 13.5 OS = 13.2

log MAR, logarithm of minimal angle of resolution; OD, oculus dexter (right eye); OS, oculus sinister (left eye); OU, oculus uterque (both eyes); wnl, within normal limits; FR, foveal reflex; IS/OS, inner segment/outer segment junction of the photoreceptors; RPE, retinal pigment epithelium; ND, nondetectable; SD-OCT, spectral-domain optical coherence tomography; AO, adaptive optics; MP, microperimetry; N/A, not available.

therefore, an equation width >5 units was considered to be abnormal.[27] The most frequent average midpoint, as provided by the manufacturer, is a red green ratio setting of 40, with a range of 34–46.

OCT Examination Protocols

All subjects included in the study underwent OCT examinations by using either a Fourier-domain (FD-OCT) system (RTvue, Optovue Technology, version 3.5; Optovue Inc., Fremont, CA) or an SD-OCT/scanning laser ophthalmoscope (SLO) system (OPKO Instrumentations, Miami, FL).

The examination protocols used for scanning the macula were as follows: in the first system (Optovue), the MM5 and radial lines protocols were used for image acquisition, where the radial scan consisted of 12 radial scans (6-mm) at 15° polar intervals passing through the center of the fovea. All 12 scans were acquired simultaneously, and the total time taken for their acquisition was 0.27 second. Each radial line consisted of 1024 A-scans. The MM5 scan protocol consisted of a raster protocol of 5 × 5 mm centered at the fovea, with a total acquisition time of 0.78 second. Scans were accepted only if they had a signal strength index >35 and were free of artifacts.

For the second system (OPKO), both the line scan (B-scan) and the three-dimensional (3D) retinal topography scan protocols were used for image acquisition. The line scan mode allows the capture of high-resolution cross-sectional B-scan OCT images of the vitreoretinal, retinal, and chorioretinal structures. The 3D retinal topography mode covers an area of 9.0 × 9.0 mm with a 2.0-mm depth.

The retinal thickness map is displayed as nine ETDRS-like subfields including central, parafoveal and perifoveal superior, temporal, inferior, and nasal subfields. The central subfield included the circle centered on the fovea with a radius of 0.5 mm. The parafoveal subfields included the concentric ring of retina around the central subfield with an inner radius of 0.5 mm and an outer radius of 1.5 mm from the fovea. The perifoveal subfields included the outer ring of retina beyond the parafoveal subfields concentric with the fovea and with an inner radius of 1.5 mm and an outer radius of 3 mm. The macular thickness data were compared with normative data provided by the manufacturers, comprised of 225 eyes of 119 normative control subjects (mean age of 47.8 ± 16.3 years) for the second (OPKO) system and 268 eyes of 134 normative control subjects (mean age of 44.1 ± 15.5 years) for the first (Optovue) system. The data acquired by both system OCTs (Optovue and OPKO) were used for analysis in the present study. All patients were able to perform the examination without any difficulty either due to a nystagmus that was mild in most of the patients or photoaversion problems.

For nine subjects, during AO imaging at the Medical College of Wisconsin, additional images of the macula were obtained using a high-resolution SD-OCT (Bioptigen, Inc., Durham, NC). Line scan sets were acquired (1000 A-scans/B-scan; 100 repeated B-scans) through the foveal center, and this location was confirmed based on inspection of the accompanying high-density volume scan. Scans were registered and averaged as previously described to reduce speckle noise in the image.[28]

AO Imaging

Each subject's eye was dilated and accommodation suspended using one drop each of phenylephrine (2.5%) and tropicamide (1%). Images of the central retina were obtained using one of two imaging systems housed at the Medical College of Wisconsin, either an AO flood-illuminated camera or an AO scanning laser ophthalmoscope (AOSLO). Subject 5 underwent imaging on both devices. System details for the AO camera[29] and AOSLO[30] have been previously published. The AO flood-illuminated camera operates at 167 frames/s and uses a 52-channel deformable mirror (Imagine Eyes, Orsay, France), whereas the AOSLO operates at 14 frames/s and uses a 97-channel deformable mirror (ALPAO, Biviers, France). Flood-illuminated AO images were processed according to previously published methods, with multiple images being registered and averaged to improve the image contrast.[29]

For the AOSLO, a desinusoiding algorithm was applied to each video sequence and individual frames were then selected for analysis. No filtering of any kind was applied to these images. From these processed images, rod and cone density was estimated using a direct counting procedure.[31,32] In all cases, the approximate retinal location of the photoreceptor images relative to the foveal center was determined based on the fundus images using common blood vessel patterns and the subjects' suspected locus of fixation (derived from the volumetric OCT images).

Macular Sensitivity Testing by MP

MP was performed on four patients with achromatopsia using the spectral OCT/SLO MP system (OPKO Instrumentations). This instrument allows the examiner to view the fundus on a computer monitor while it is imaged in real time by the SLO fundus camera. Background luminance was set at 10 cd/m². Stimulus intensity can be varied in 1 dB (0.1 log) steps from 0 to 20, where 0 dB represents the brightest luminance of 125 cd/m². The system also incorporates an automated tracking system to compensate for eye movement during examination.

The testing was conducted in a darkened room that minimized the photoaversion commonly experienced by patients with achromatopsia. All patients underwent brief training at the beginning of MP testing, allowing familiarization and practice with correct operation of the response trigger and the stimulus target. This was followed immediately by the actual test. All tests were performed after pupil dilatation. Patching of the nontested eye was performed. The patients were instructed to fixate on a red square as a fixation target and press a button once they saw the stimulus target. A standard grid pattern (Polar 3), composed of 28 points arranged in three concentric circles (2.3°, 6.6°, and 11° in diameter) within the central macula, was used. The inner circle is composed of four points, whereas the middle and outer circles are each composed of 12 points. Parameters included a stimulus (Goldmann III size), 200-ms stimulus duration, and test strategy 4-2. The individual sensitivity values at 28 different loci within the central 12° were compared with normative data, which were retrieved from 32 visually normal subjects.[33]

Molecular Analysis

For subjects 1 to 5 and 7 to 9 (Table 2), DNA was isolated from whole blood and used in the polymerase chain reaction (PCR) in the Neitz Laboratory at the Medical College of Wisconsin, or at the University of Washington. Mutation screening was performed on exons and intron/exon junctions of the genes encoding the α-subunit of cone transducin (*GNAT2*), and the genes encoding the α-subunit (*CNGA3*) and β-subunit (*CNGB3*) of the cone cyclic nucleotide-gated ion channel. Exon 18 of the *CNGB3* was not analyzed. Individual exons or pairs of adjacent exons and the intron/exon junctions for each gene were amplified, and both strands of the resulting PCR products were directly sequenced. Sequencing was performed using a commercial kit (AmpliTaq FS kit; PerkinElmer, Waltham, MA) and reactions were analyzed on a genetic analyzer (ABI 3130xls; Applied Biosystems/Life Technologies Corp., Carlsbad, CA).

For subjects 1 to 5 and 7 to 9, independent genetic analysis was conducted by the Carver Laboratory at the University of Iowa on the exons for the *CNGA3* and *CNGB3* genes. Additionally, DNA from blood samples was obtained from subjects 6 and 10 to 12 and analyzed in the Carver Laboratory; DNA was extracted by following the manufacturer's specifications for whole blood DNA extraction using a commercial instrument (Gentra Systems Autopure LS). Automated bidirectional DNA sequencing of the coding sequences of *CNGA3* and *CNGB3* was performed using a commercial sequencer (ABI 3730; Applied Biosystems). Exon 18 of the *CNGB3* gene was sequenced for all subjects in the Carver Laboratory.

TABLE 2. Summary of Screening Results of Genetic Mutations in the Study Cohort

Patient Number	Age (y)/ Sex	Race/Ethnicity	Gene	Allele 1	Allele 2
1	13/F	Hispanic	No mutations found		
2	15/M	Caucasian	*CNGA3* exons 6 and 7, heterozygous	c.661C>T–p.Arg221Stop	c.830G>A–p.Arg277His
3	30/F	Caucasian	*CNGB3* exon 10, heterozygous	c.1148delC–p.Thr383fs	Not found
4	50/M	Lebanese	*CNGA3* exon 7, homozygous	c.1709G>T–p.Ser570Ile	c.1709G>T–p.Ser570Ile
5	15/M	Caucasian	*CNGB3* exon 10, homozygous	c.1148delC–p.Thr383fs	c.1148delC–p.Thr383fs
6	17/F	Jordanian	*CNGA3* exon 7, heterozygous	c.985G>T–p.Gly329Cys	c.1306C>T–p.Arg436Trp
7	27/F	Caucasian	*CNGB3* exon 10, homozygous	c.1148delC–p.Thr383fs	c.1148delC–p.Thr383fs
8	49/M	Caucasian	*CNGB3* exon 10, homozygous	c.1148delC–p.Thr383fs	c.1148delC–p.Thr383fs
9	33/M	Hispanic	*CNGA3* exon 7, heterozygous	c.1228C>T–p.Arg410Trp	c.1541A>T–p.Asp514Val
10	55/M	Caucasian	*CNGB3* exon 10, heterozygous	c.1148delC–p.Thr383fs	Not found
11	52/F	African American	*CNGA3* exon 7, heterozygous	c.848G>A–p.Arg283Gln	c.1306C>T–p.Arg436Trp
12	14/M	Jordanian	*CNGA3* exon 7, heterozygous	c.985G>T–p.Gly329Cys	c.1306C>T–p.Arg436Trp

DNA numbering is based on cDNA sequence (GenBank: AF065314.1); nucleotide +1 is the A of the start codon (ATG).

RESULTS

Clinical Examination

The average BCVA was 0.88 logMAR units with SD of 0.14 (range, 0.44–0.96), equivalent to 20/55 to 20/186 on a Snellen acuity chart. Subjectively, all patients had a past history of pendular nystagmus dated since birth that improved over time. The degree of photoaversion was mild in 2 patients and moderate to severe in 10 patients.

Fundus examination in our study cohort showed 3 patients (25.0%) with a normal macular morphology and normal-appearing foveal reflex (mean age, 14.7 years; range, 13 to 17 years), 5 patients (41.7%) showed a blunted (absent) foveal reflex (mean age, 28.6 years; range, 15 to 50 years), and 2 patients (16.7%) showed evidence of macular lesions in the form of retinal pigment epithelium (RPE) mottling, mild hypopigmentary changes in the fovea/parafoveal regions, or a few, punctate, hard drusen in each eye (ages 27 and 55 years). In addition, 2 patients (16.7%) showed a well-circumscribed atrophic-appearing macular lesion in each eye (ages 49 and 52 years) (Table 1).

Genetic Analysis

Our genetic testing results showed that 11 of 12 patients had a positive genetic mutation in either the *CNGB3* or *CNGA3* gene, which was similar to previous reports.[8,34,35] Mutations were independently confirmed in the Carver Laboratory and Neitz Laboratory for subjects 1 to 5 and 7 to 9. The other subjects were sequenced only in the Carver Laboratory. The genetic results are summarized in Table 2.

The achromatopsia phenotype for subjects 5, 7, and 8 can be attributed to each of these subjects being homozygous for a frame-shift mutation in exon 10 of the *CNGB3* gene in which residue C 1148 in codon 383 is deleted.[4,8] Subject 4 is homozygous for a missense mutation in the *CNGA3* gene at codon 570 (Ser570Ile). Subjects 2, 6, 9, 11, and 12 are each compound heterozygotes for two different mutations within the *CNGA3* gene. For subject 2, one mutation changes codon 221 from arginine to a premature translational termination codon; the second mutation is a previously identified pathogenic missense mutation (Arg277His).[7] Subjects 6 and 12 were found to have a new mutation (Gly329Cys) and a previously identified mutation (Arg436Trp).[4,7,36] Subject 9 has two different missense mutations in the cGMP binding domain of *CNGA3*. These include a new mutation (Asp514Val) and a previously identified mutation, (Arg410Trp).[4,7,36] Subject 11 has two previously described mutations, Arg283Gln and Arg436Trp.[4,7,36] Subjects

3 and 10 are both heterozygous for the one base deletion at position 1148 of the *CNGB3* gene, although a second mutation was not found in *CNGB3* or *CNGA3* for either subject or in the *GNAT2* gene for subject 3. The *GNAT2* gene was not evaluated for subject 11. For subject 1, clearly pathogenic mutation(s) in *CNGA3*, *CNGB3*, or *GNAT2* were not found.

Color Vision Results

Color vision screening with color plates (Ishihara) showed the ability to identify only the test plate in six patients (50.0%), whereas six patients (50.0%) could identify plates from 1 to 5. Anomaloscopic examination showed an abnormality consisting most commonly of a shift of the Rayleigh match midpoint toward the red end of the color spectrum, with an average midpoint of 54 and an abnormal equation width in seven patients (58.3%), whereas five patients (41.7%) matched at the entire range of the anomaloscope from 0 to 73. The red–green half of the anomaloscopic field appeared dim at longer wavelengths and substantially brighter at shorter wavelengths in most of the study patients ($n = 9$).

Assessing Photoreceptor Function: ERG Findings

Full-field ERG recordings were obtained on all the study patients. The isolated rod response was normal in 9 patients (75.0%) with an average amplitude of 387.7 μV (lower limit of normal is 273 μV), whereas 3 patients (25.0%) showed an average reduction of 31% below the lower limit of normal with an average amplitude of 187.3 μV. The maximum dark-adapted response after 30 minutes was normal in 6 patients (50.0%), with an average amplitude of 559.8 μV (lower limit of normal is 460.9 μV), whereas 6 patients (50.0%) showed an average reduction of 24% below the lower limit of normal with an average amplitude of 351.4 μV. The single-flash light-adapted response was nondetectable in 2 patients (16.7%), whereas 10 patients (83.3%) showed a markedly reduced b-wave response with average amplitude of 34.9 μV (lower limit of normal is 132.8 μV). All patients showed nondetectable responses to a 32-Hz flicker stimulus.

MP Results

Macular MP testing was performed on 8 eyes of 4 patients (mean age, 19.0 years; range, 14 to 30 years), and the results were compared with 32 visually normal subjects (mean age, 41.6 years; range, 28 to 66 years) on the same SD-OCT/SLO system used in this study.[33]

The MP testing showed that the overall mean retinal sensitivity in our currently studied patients was significantly less

than that of controls (12.0 vs. 16.9 dB, $P < 0.0001$; Student's *t*-test was used for statistical analysis). MP testing of 28 individual points within a 6° radius from the center of the foveola (12° circle, Polar 3 pattern) showed areas of subnormal individual point sensitivities that were below the 95 and 99% confidence limits of normal sensitivity. In addition, the four patients studied showed relatively stable central fixation in each eye (81% of eye movements were within 2° around the projected fixation target, whereas 92% were within 4°) (Fig. 1). The structural and functional characteristics of these four patients are shown in Table 1.

Retinal Morphology in Achromatopsia: SD-OCT Results

Regarding the SD-OCT examination, two patients (16.7%) (ages 13 and 17 years) showed normal macular structures, with an

FIGURE 1. Correlating SD-OCT and MP findings from two patients with achromatopsia (subjects 2 and 3). Shown are isolated patchy areas of subnormal retinal thresholds within the posterior pole compared with previously published normative data.[33]

intact IS/OS junction of the photoreceptors and grossly normal appearing outer nuclear layer (ONL) thickness. Six patients (50.0%) showed a shallow and broad foveal depression (possibly reflecting a degree of foveal hypoplasia or maldevelopment)[32] with continuation of the inner plexiform layer (IPL) and outer plexiform layer (OPL) to within the foveolar region (Fig. 2). Ten patients (83.3%) showed focal disruption and/or loss of the IS/OS junction of the photoreceptors and RPE layer attenuation within the macular region (mean age, 34.0 years; range, 14 to 55 years). Seven of those 10 patients showed the presence of an optically empty space (punched-out hyporeflective space) at the level of IS/OS junction of the photoreceptors that corresponded to disruption and/or loss of the photoreceptor layer (Fig. 2).

By a quantitative method of analysis, on OCT examination, 11 eyes (45.8%) of 6 patients showed a normal central foveal subfield thickness, with an average thickness of 259.0 ± 11.7 μm (mean age, 22.7 years; range, 13 to 50 years). Thirteen eyes (54.2%) of 7 patients showed thinning in the central foveal subfield, with an average thickness of 193.8 ± 25.7 μm (mean age, 32.8 years; range, 14 to 55 years), which was significantly thinner statistically than normal ($P < 0.0001$; Student's *t*-test was used for statistical analysis). The data used for measurement of the macular thickness were obtained from both systems (Optovue and OPKO).

Photoreceptor Structure Assessed with AO Imaging

The AO images of the photoreceptor mosaic were highly variable, both in image quality and in the appearance of the mosaic itself. In all cases, the mosaic was significantly disrupted from normal (Fig. 3). In the normal retina, peripheral cones appear as bright spots with a dark ring and, in some cases, this central bright spot is missing (arrows, panel b). We posit that the dark ring is the inner segment of the cone, whereas the central reflection is derived from the outer segment or IS/OS junction. These images are critical to interpreting the findings in patients with achromatopsia, as we observed residual cone inner segment structure in all but one of the subjects imaged. In fact, in three individuals (subjects 5, 10, and 12 in Table 2) we found cones that had a subtle central reflective structure within the inner segment, suggesting improved structural integrity of the outer segment relative to the other patients. It may be that the presence/absence of this structure, or its intensity, could be an indicator of relative cone structural health.

We were able to acquire images at approximately 10° from the fovea in two subjects (Figs. 3D, 3E), and found quite different degrees of residual cone structure, although both appeared reduced compared with the normal image at 10° from the fovea (Fig. 3B). In all images, the cross-sectional profiles of individual rods and cones appeared consistent with that previously reported.[25] In one subject (subject 5 in Table 2) we were able to map the border of his central IS/OS disruption (see Fig. 4). Given the size of the disruption (201 μm), we believe that this represents the rod-free zone in this individual because it is consistent with previous estimates of this structure.[37]

In another subject (subject 12 in Table 2) we were able to examine multiple locations of known distance from the fovea. Although no obvious cone structure could be seen in the central fovea, cone inner segments were present at 2, 4, and 16° eccentricity, although they were least numerous at 16° (Fig. 5).
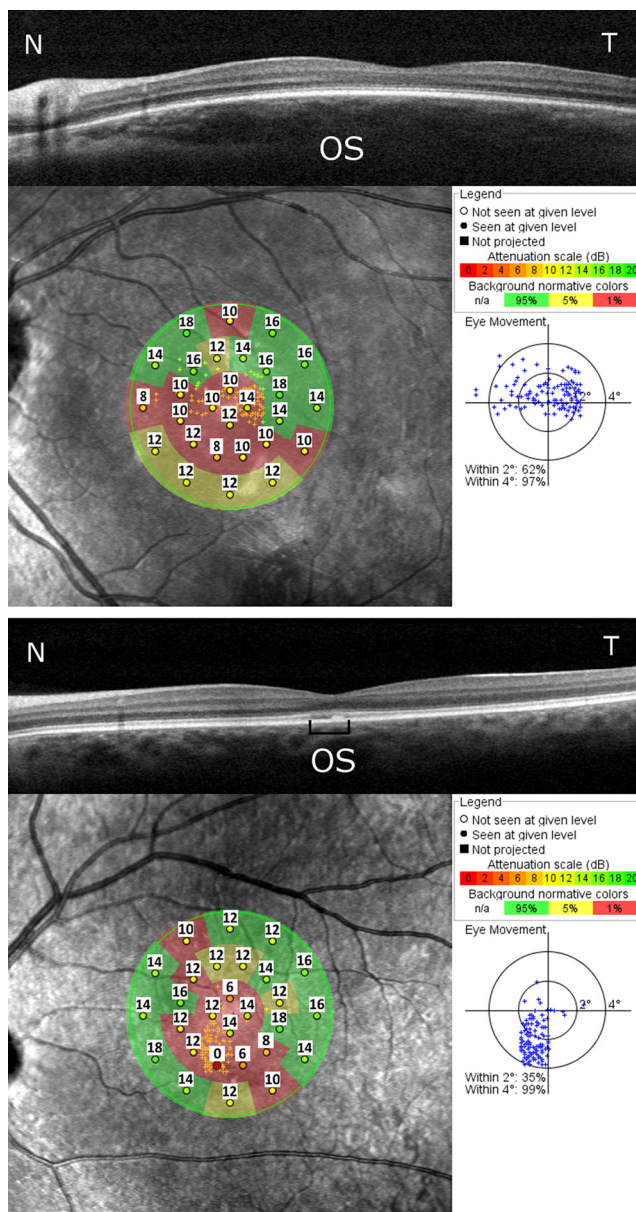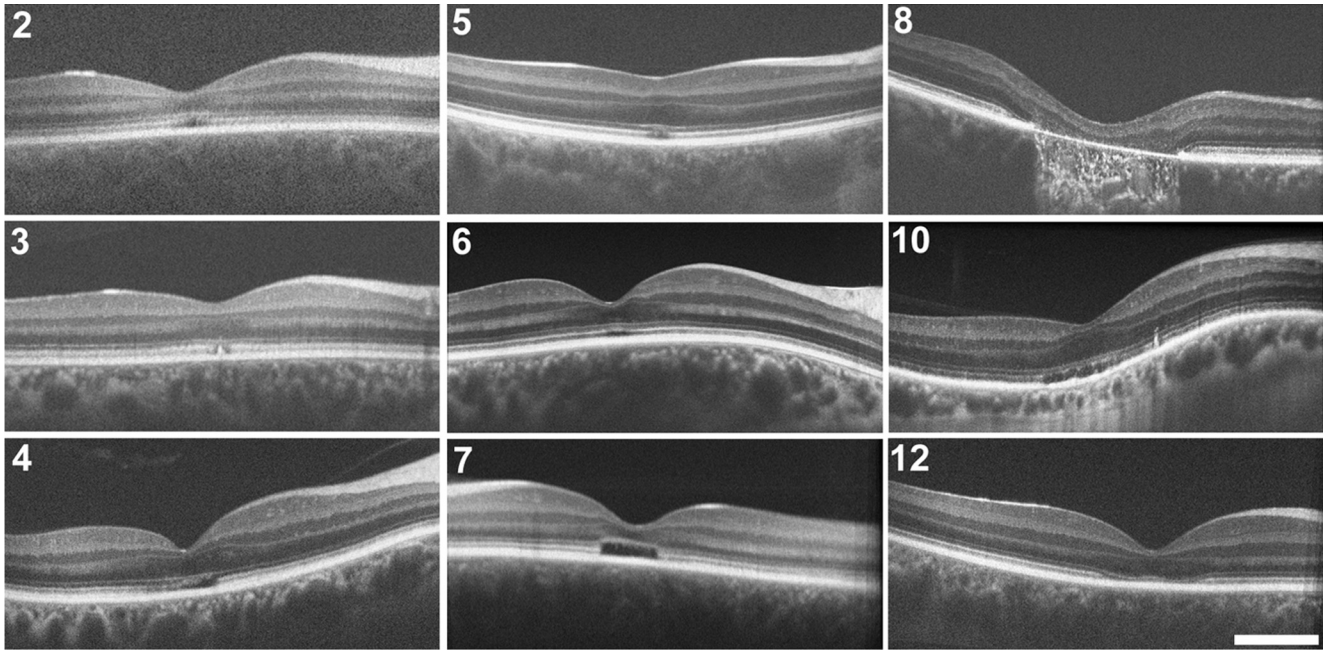
FIGURE 2. High-resolution SD-OCT scans through the fovea. Scans were acquired using the Bioptigen SD-OCT and foveal location was confirmed using accompanying volume scans. Panel numbers correspond to subject numbers in Table 1. Note the variable appearance of the IS/OS disruption in these individuals, even in subjects with the same genotype (subjects 5, 7, and 8 and subjects 6 and 12). Scale bar, 1 mm.

DISCUSSION

Macular Structure in Achromatopsia

We used a variety of techniques to assess macular structure in patients with achromatopsia. The value of fundus imaging techniques in assessing patients with achromatopsia has been described in previous studies.[6,20,21,25] In our study cohort of 12 patients afflicted with achromatopsia, 7 patients (58.3%) showed evidence of minor macular changes on fundus examination that varied from either an absent foveal reflex or non-
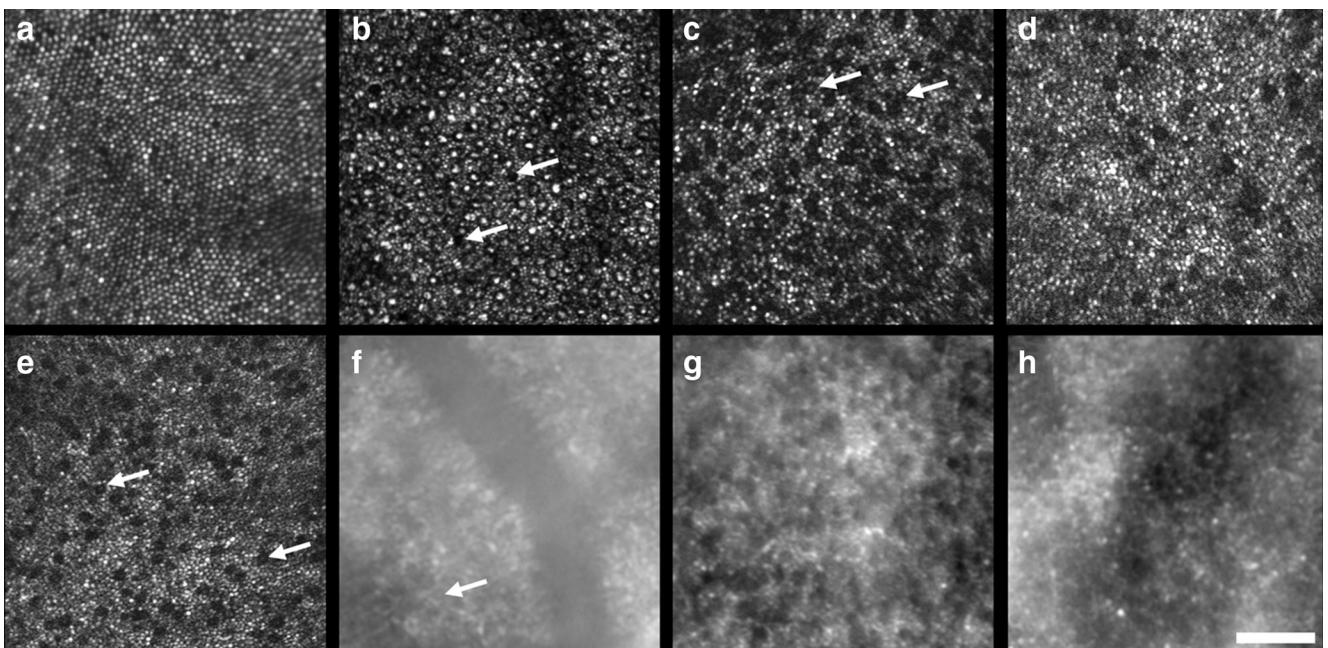

FIGURE 3. Images of the photoreceptor mosaic in achromatopsia. Images of the foveal cone mosaic (**a**) and peripheral (~10°) rod and cone mosaic (**b**) obtained with the AOSLO for a normal subject are shown for comparison. In the peripheral image, the dark ring associated with each cone is presumably the boundary of the inner segment, whereas the central reflective core is from the outer segment or IS/OS junction. Note the variable appearance of the cones in the normal retina (**b**), with some cones being devoid of a central reflection (*arrows* in **b**). The images in (**c–e**) represent individual frames from the AOSLO, whereas (**f–h**) are from the AO flood-illuminated camera. All subjects had evidence of residual cone structure, although to a variable degree. (**c**) and (**g**) are from subject 5, (**d**) is from subject 8, (**e**) is from subject 12, (**f**) is from subject 10, and (**h**) is from subject 6. (**c–f**) demonstrate the presence of multiple cone inner segments that still retain a central reflective core (*arrows*), although it is diminished in its reflectance compared with normal. Scale bar, 50 μm.
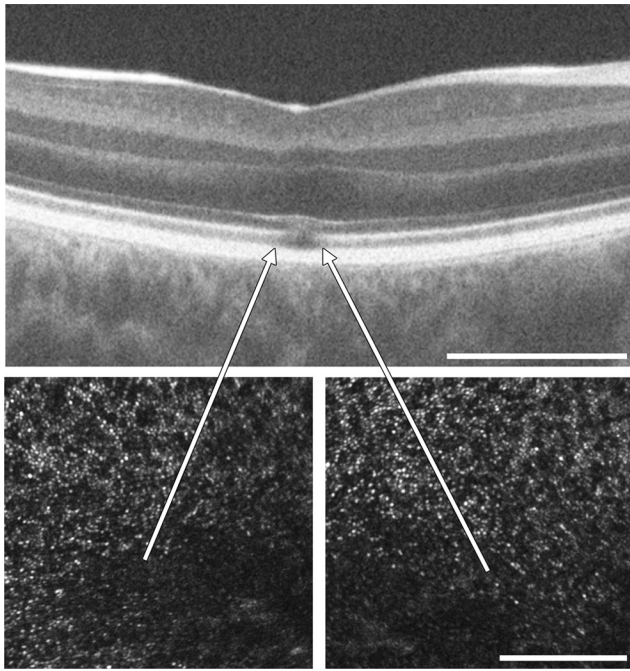
FIGURE 4. Correlating SD-OCT and AOSLO findings. Shown is a section of the SD-OCT scan for subject 5, and corresponding AOSLO images from either side of the focal IS/OS disruption. Scale bars are 1 mm (SD-OCT) and 100 μm (AOSLO). The extent of this disruption (approximately 200 μm) is consistent with the reported size of the rod-free zone.[37]

specific RPE mottling to mild hypopigmentary changes. Two patients showed a well-circumscribed atrophic-appearing macular lesion, whereas 3 patients did not show any clinically apparent macular changes. These findings were similar to two recent reports[4,34] that showed macular changes in achromatopsia patients.

Three anatomic features of the macula can be examined using SD-OCT imaging: the appearance of the photoreceptor layer (external limiting membrane and IS/OS), macular thickness, and foveal morphology. Our findings were generally consistent with previous reports, adding to the current picture of significant structural variability in patients with achromatopsia. Ten patients in our cohort showed a disruption or loss of the IS/OS junction of the photoreceptors in the macula. The presence of an optically empty space (punched-out hyporeflective space) at the level of the photoreceptors in the fovea was observed in seven patients (mean age, 32.1 years). This has been observed previously by others in patients in which no genetic subtype was identified.[6,11,38] The exact mechanisms for the foveal optically empty space and disrupted IS/OS junction of the photoreceptor layer are not currently known. One hypothesis is that they might be due to autolysis of cone photoreceptor outer segments or ineffective phagocytosis of degenerative photoreceptor cell debris.

In contrast, two of the younger patients (ages 13 and 17 years) showed a normal macular structure with a generally intact IS/OS junction of the photoreceptors and normal-appearing ONL thickness. This general difference in IS/OS structure is consistent with the findings presented by Thiadens et al.,[6] who reported loss of the IS/OS junction with a disruption of the ciliary layer (the connecting cilium of the photoreceptors) on OCT initially, followed by the appearance of an evolving bubble in the photoreceptor layer and thinning or atrophic-appearing changes of the RPE in older patients with achromatopsia. Eleven eyes (45.8%) of six patients showed a normal foveal subfield thickness, whereas 13 eyes (54.2%) of seven patients showed a thinning of the foveal subfield thickness on OCT examination. This variability is consistent with findings reported previously[6,20,21] and may arise from differences in age and/or genotype. Six of our patients had a broad and shallow foveal depression with preservation of inner retinal layers through the foveal center, similar to that seen in some individuals with albinism.[32] Foveal hypoplasia is recognized as a relatively common feature of achromatopsia,[4,6,35] although the significance of this finding as it pertains to the etiology of achromatopsia remains to be defined.

AO permits direct visualization of individual rod and cone photoreceptors.[39,40] It is becoming appreciated that in a variety of diseases, AO can reveal cellular disruption in areas that appear normal with conventional imaging tools (including SD-OCT) (Stepien KE, et al. *IOVS* 2011;52:ARVO E-Abstract 6657).[41,42] We directly examined photoreceptor structure in nine subjects using AO, and observed residual cone inner segment structure in all but one of the subjects imaged. In three individuals (subjects 5, 10, and 12) we even observed cones that had a subtle central reflective structure within the inner segment, suggesting improved structural integrity of the outer segment relative to that of the other patients. The variable appearance of the residual cones may be an indicator of relative cone structural health, although this requires further investigation. That we see cone structure even in the oldest patient (55 years old) suggests that, although there may be general advancement of the disease with age, there is not a complete loss of cone structure. Thus the therapeutic window may be larger than that inferred from recent SD-OCT studies.[6] Interestingly, there was nothing unique about these three subjects' SD-OCT images, highlighting that it may not be possible to directly infer the degree of cone structure from SD-OCT imaging alone. This was perhaps most notable in subject 12, where in areas that lacked a robust IS/OS layer, we still observed numerous cone IS structures. It would be of interest to image with AO individuals receiving gene therapy intervention because AO imaging (specifically the appearance of the cone reflection profile) may provide the most sensitive biomarker for assessing a treatment response in patients receiving therapeutic intervention for achromatopsia. In addition, in future longitudinal studies, it would be useful to assess how cone structure changes over time with AO and SD-OCT.

Residual Cone Function in Achromatopsia

We observed significant residual cone function in our patients, albeit to a variable degree. Regarding color vision (a cone-mediated process), only 5 of the 12 patients matched the entire range of red green mixtures on the anomaloscope, whereas 7 patients showed a midpoint shifted toward the red end of the Rayleigh match, which has been reported previously in incomplete achromatopsia.[43] Of those 5 patients who matched over the entire range of the anomaloscope, all patients showed a nondetectable (ND) light-adapted flicker response, 2 of the 5 patients showed an ND single-flash light-adapted response, whereas 3 patients showed an average b-wave amplitude of 35.9 μV to a single-flash light-adapted response, with a lower limit of normal of 132.8 μV. Of those patients who showed a shift in their match point into the red portion of the color spectrum ($n = 7$), all showed ND responses to the flicker stimulus, whereas all patients showed residual cone function to the single-flash light-adapted stimulus, with an average of 32.9 μV and a range of 26.0 to 43.0 μV (lower limit of normal is 132.8 μV). Regarding the photopic ERG in our entire study cohort, 10 patients (83.3%) showed evidence of residual cone responses to a single-flash stimulus response, whereas all patients showed ND responses to a flicker stimulus. In addition,
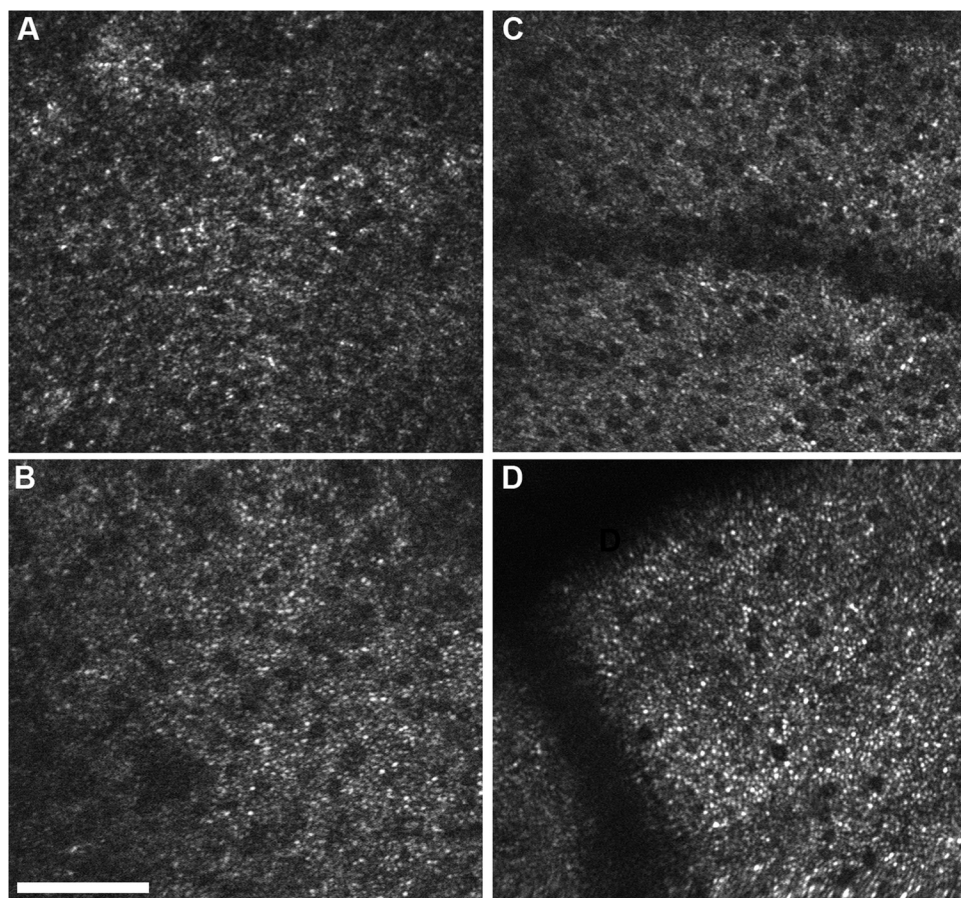
FIGURE 5. Images of the photoreceptor mosaic at different eccentricities. All four images are from subject 12, and were taken from the central fovea (**A**), 2° (**B**), 4° (**C**), and 16° (**D**). Retinal location was determined based on blood vessel appearance in neighboring AOSLO video frames. There is an absence of obvious cone structure in the central fovea, consistent with observations on SD-OCT. However, the number of cone inner segments increases at the 2° location, before falling off in the more peripheral locations. Scale bar, 100 μm.

the rod responses were normal in 9 patients, whereas 3 patients showed an average of an almost 31% reduction below the lower limit of normal, which was similar to a previous report by Khan et al.,[2] who showed an abnormality of scotopic ERG responses in patients with achromatopsia. Finally, the mean sensitivity on macular MP of 12.0 dB is consistent with the presence of residual cone function. Taken together, these functional findings further support the notion that patients with achromatopsia can have substantial residual cone function, which is in accordance with prior reports.[4,5]

Genotype Phenotype Correlations in Achromatopsia

Prior reports showed that mutations in the *CNGA3* and *CNGB3* genes are the most frequent mutations encountered in patients with achromatopsia.[8,38,44] Consistent with this, disease-causing mutations in *CNGA3* and *CNGB3* genes were observed in 11 of 12 of our patients. A limitation of the present study is the relatively small number of subjects and the diverse genotypes (including an absence of disease-causing mutations in one patient), making it impossible to draw firm conclusions about genotype phenotype relationships. That said, we did not observe any distinguishing clinical, psychophysical, electrophysiological, or structural (SD-OCT/AO) features in patients with *CNGB3* versus *CNGA3* mutations. None of our patients was found to have a mutation(s) in the *GNAT2* gene, so it remains unclear whether such patients might show any systematic differences in cone structure and function. The unifying finding is that there is substantial variation in phenotype, even within individuals with the same genotype. Three unrelated patients in our study (subjects 5, 7, and 8 in Tables 1 and 2; ages 15, 27, and 49 years, respectively) showed the same

homozygous mutation in the *CNGB3* gene, although their phenotypic findings differed. The 15-year-old patient showed a normal-appearing fundus examination and ND cone responses to both single-flash light-adapted and 32-Hz flicker stimuli with normal rod response on ERG testing. The 27-year-old patient showed a foveal hypopigmented lesion and ND (to 32-Hz flicker) and markedly reduced (to single-flash light-adapted) cone responses with normal rod responses on ERG testing, whereas the 49-year-old patient showed an atrophic-appearing macular lesion on fundus examination and ND (to 32-Hz flicker) and markedly reduced (to single-flash light-adapted) cone responses with normal rod responses on ERG testing. Two of our study patients are siblings (subjects 6 and 12 in Tables 1 and 2, ages 17 and 14 years, respectively) and carry the same heterozygous mutations in the *CNGA3* gene without any differences in their phenotype, both clinically and electrophysiologically. However, subject 12 showed more loss of foveal IS/OS junction of the photoreceptors than that of his older sister (subject 6) on OCT testing (Fig. 1). Since our study was not intended to identify longitudinal changes in either retinal structure or function in our patients, we cannot meaningfully address whether any of our differences between individuals with the same genotype support or refute the proposed progressive degeneration reported by Thiadens et al.[6] or whether they represent the effect of an unidentified modifying factor. The issue of progressive loss of cones in achromatopsia remains an important unresolved issue, and will be settled with additional longitudinal imaging studies only on patients of known genotype and/or much larger cross-sectional studies.

Our findings are generally consistent with those reported by Nishiguchi et al.,[4] who reported residual cone structure in all patients with achromatopsia they examined, but found no

obvious correlation between the specific genotype and the severity of cone dysfunction. In addition, subjects 5 (*CNGB3*) and 12 (*CNGA3*) had more substantial cone structure in their AO images, with many cones containing a reflective core (presumed OS in origin). This demonstrates that significant cone structure can remain in the two main genotypes, although further work is needed to determine whether there is any significant difference between individuals harboring different mutations within each genotype. Taken together, these findings indicate that genetic analysis alone may not be sufficient to identify the best candidates for a given gene therapy intervention.

Implications for Improving the Success of Gene Therapy in Humans

In studies of animal models of human achromatopsia, AAV-mediated gene therapy was shown to recover cone ERG amplitudes to near normal levels.[12–14] There is justified enthusiasm surrounding the prospect of translating these proof-of-principle experiments in animals to the treatment of human patients. We feel that the combined assessment of photoreceptor structure and function outlined here will be important to ultimately improving the success of such intervention and help to identify the best candidates for a specific therapy. For example, in a group of patients with retinitis pigmentosa, Talcott et al.[45] recently demonstrated that imaging of the cone mosaic with AOSLO showed improvements in cone structure in response to ciliary neurotrophic factor treatment that were not visible using conventional assays. We anticipate that application of similar high-resolution imaging techniques and sensitive measures of retinal function will provide a more sensitive evaluation of therapeutic efficacy in clinical trials for patients with achromatopsia.

References

1. Sharpe LT, Stockman A, Jagle H, et al. Opsin genes, cone photopigments and colour blindness. In: Gegenfurtner K, Sharpe LT, eds. *Color Vision: From Genes to Perception.* Cambridge, UK: Cambridge University Press; 1999:3–52.

2. Khan NW, Wissinger B, Kohl S, Sieving PA. CNGB3 achromatopsia with progressive loss of residual cone function and impaired rod-mediated function. *Invest Ophthalmol Vis Sci.* 2007;48:3864–3871.

3. Pokorny J, Smith VC, Pinckers AJ, Cozijnsen M. Classification of complete and incomplete autosomal recessive achromatopsia. *Graefes Arch Clin Exp Ophthalmol.* 1982;219:121–130.

4. Nishiguchi KM, Sandberg MA, Gorji N, et al. Cone cGMP-gated channel mutations and clinical findings in patients with achromatopsia, macular degeneration, and other hereditary cone diseases. *Hum Mutat.* 2005;25:248–258.

5. Michaelides M, Hardcastle AJ, Hunt DM, Moore AT. Progressive cone and cone-rod dystrophies: phenotypes and underlying molecular genetic basis. *Surv Ophthalmol.* 2006;51:232–258.

6. Thiadens AA, Somervuo V, van den Born LI, et al. Progressive loss of cones in achromatopsia: an imaging study using spectral-domain optical coherence tomography. *Invest Ophthalmol Vis Sci.* 2010; 51:5952–5957.

7. Wissinger B, Gamer D, Jägle H, et al. CNGA3 mutations in hereditary cone photoreceptor disorders. *Am J Hum Genet.* 2001;69: 722–737.

8. Kohl S, Baumann B, Broghammer M, et al. Mutations in the CNGB3 gene encoding the beta-subunit of the cone photoreceptor cGMP-gated channel are responsible for achromatopsia (ACHM3) linked to chromosome 8q21. *Hum Mol Genet.* 2000;9:2107–2116.

9. Chang B, Dacey MS, Hawes NL, et al. Cone photoreceptor function loss-3, a novel mouse model of achromatopsia due to a mutation in Gnat2. *Invest Ophthalmol Vis Sci.* 2006;47:5017–5021.

10. Rosenberg T, Baumann B, Kohl S, Zrenner E, Jorgensen AL, Wissinger B. Variant phenotypes of incomplete achromatopsia in two cousins with GNAT2 gene mutations. *Invest Ophthalmol Vis Sci.* 2004;45:4256–4262.

11. Thiadens AAHJ, den Hollander AI, Roosing S, et al. Homozygosity mapping reveals PDE6C mutations in patients with early-onset cone photoreceptor disorders. *Am J Hum Genet.* 2009;85:240–247.

12. Komáromy AM, Alexander JJ, Rowlan JS, et al. Gene therapy rescues cone function in congenital achromatopsia. *Hum Mol Genet.* 2010;19:2581–2593.

13. Alexander JJ, Umino Y, Everhart D, et al. Restoration of cone vision in a mouse model of achromatopsia. *Nat Med.* 2007;13:685–687.

14. Carvalho LS, Xu J, Pearson RA, et al. Long-term and age-dependent restoration of visual function in a mouse model of CNGB3-associated achromatopsia following gene therapy. *Hum Mol Genet.* 2011;20:3161–3175.

15. Galezowski X. *Du diagnostic des Maladies des Yeux par la Chromatoscopie rétinienne: Précéde d'une Etude sur les Lois physiques et physiologiques des Couleurs* [in French]. Paris: J.B. Baillière et Fils; 1868.

16. Larsen H. Demonstration mikroskopischer Präparate von einem monochromatischen Auge [in German]. *Klin Monatsbl Augenheilkd.* 1921;67:301–302.

17. Harrison R, Hoefnagel D, Hayward JN. Congenital total color blindness: a clinicopathological report. *Arch Ophthalmol.* 1960; 64:685–692.

18. Falls HF, Wolter R, Alpern M. Typical total monochromasy: a histological and psychophysical study. *Arch Ophthalmol.* 1965;74: 610–616.

19. Glickstein M, Heath GG. Receptors in the monochromat eye. *Vision Res.* 1975;15:633–636.

20. Barthelmes D, Sutter FK, Kurz-Levin MM, et al. Quantitative analysis of OCT characteristics in patients with achromatopsia and blue-cone monochromatism. *Invest Ophthalmol Vis Sci.* 2006;47: 1161–1166.

21. Varsányi B, Somfai GM, Lesch B, Vámos R, Farkas A. Optical coherence tomography of the macula in congenital achromatopsia. *Invest Ophthalmol Vis Sci.* 2007;48:2249–2253.

22. Liang JZ, Williams DR, Miller DT. Supernormal vision and high-resolution retinal imaging through adaptive optics. *J Opt Soc Am A.* 1997;14:2884–2892.

23. Roorda A. Applications of adaptive optics scanning laser ophthalmoscopy. *Optom Vis Sci.* 2010;87:260–268.

24. Godara P, Dubis AM, Roorda A, Duncan JL, Carroll J. Adaptive optics retinal imaging: emerging clinical applications. *Optom Vis Sci.* 2010;87:930–941.

25. Carroll J, Choi SS, Williams DR. In vivo imaging of the photoreceptor mosaic of a rod monochromat. *Vision Res.* 2008;48:2564–2568.

26. Marmor MF, Holder GE, Seeliger NW, Yamamoto S. Standard for clinical electroretinography (2003 update). *Doc Ophthalmol.* 2004;108:107–114.

27. Krill AE, Fishman GA. Acquired color vision defects. *Trans Am Acad Ophthalmol Otolaryngol.* 1971;75:1095–1111.

28. Tanna H, Dubis AM, Ayub N, et al. Retinal imaging using commercial broadband optical coherence tomography. *Br J Ophthalmol.* 2010;94:372–376.

29. Rha J, Schroeder B, Godara P, Carroll J. Variable optical activation of human cone photoreceptors visualized using a short coherence light source. *Opt Lett.* 2009;34:3782–3784.

30. Dubra A, Sulai Y. Reflective afocal broadband adaptive optics scanning ophthalmoscope. *Biomed Opt Express.* 2011;2:1757–1768.

31. Li KY, Roorda A. Automated identification of cone photoreceptors in adaptive optics retinal images. *J Opt Soc Am A Opt Image Sci Vis.* 2007;24:1358–1363.

32. McAllister JT, Dubis AM, Tait DM, et al. Arrested development: high-resolution imaging of foveal morphology in albinism. *Vision Res.* 2010;50:810–817.

33. Anastasakis A, McAnany JJ, Fishman GA, Seiple WH. Clinical value, normative retinal sensitivity values, and intrasession repeatability using a spectral-domain OCT/SLO microperimeter. *Eye.* 2011;25: 245–251.

34. Thiadens AA, Slingerland NW, Roosing S, et al. Genetic etiology and clinical consequences of complete and incomplete achromatopsia. *Ophthalmology.* 2009;116:1984–1989.

35. Thomas MG, Kumar A, Kohl S, Proudlock FA, Gottlob I. High-resolution in vivo imaging in achromatopsia. *Ophthalmology.* 2011;118:882–888.

36. Kohl S, Marx T, Giddings I, et al. Total colour blindness is caused by mutations in the gene encoding the alpha-subunit of the cone photoreceptor cGMP-gated cation channel. *Nat Genet.* 1998;19: 257–259.

37. Curcio CA, Sloan KR, Kalina RE, Hendrickson AE. Human photoreceptor topography. *J Comp Neurol.* 1990;292:497–523.

38. Grau T, Artemyev NO, Rosenberg T, et al. Decreased catalytic activity and altered activation properties of PDE6C mutants associated with autosomal recessive achromatopsia. *Hum Mol Genet.* 2011;20:719–730.

39. Rossi EA, Chung M, Dubra A, Hunter JJ, Merigan WH, Williams DR. Imaging retinal mosaics in the living eye. *Eye.* 2011;25:301–308.

40. Dubra A, Sulai Y, Norris JL, et al. Noninvasive imaging of the human rod photoreceptor mosaic using a confocal adaptive optics scanning ophthalmoscope. *Biomed Opt Express.* 2011;2:1864–1876.

41. Rha J, Dubis AM, Wagner-Schuman M, et al. Spectral domain optical coherence tomography and adaptive optics: imaging photoreceptor layer morphology to interpret preclinical phenotypes. *Adv Exp Med Biol.* 2010;664:309–316.

42. Stepien KE, Han DP, Schell J, Godara P, Rha J, Carroll J. Spectral-domain optical coherence tomography and adaptive optics may detect hydroxychloroquine retinal toxicity before symptomatic vision loss. *Trans Am Ophthalmol Soc.* 2009;107:28–33.

43. Smith VC, Pokorny J, Newell FW. Autosomal recessive incomplete achromatopsia with protan luminosity function. *Ophthalmologica.* 1978;177:197–207.

44. Wiszniewski W, Lewis RA, Lupski JR. Achromatopsia: the CNGB3 p.T383fsX mutation results from a founder effect and is responsible for the visual phenotype in the original report of uniparental disomy 14. *Hum Genet.* 2007;121:433–439.

45. Talcott KE, Ratnam K, Sundquist SM, et al. Longitudinal study of cone photoreceptors during retinal degeneration and in response to ciliary neurotrophic factor treatment. *Invest Ophthalmol Vis Sci.* 2011;52:2219–2226.